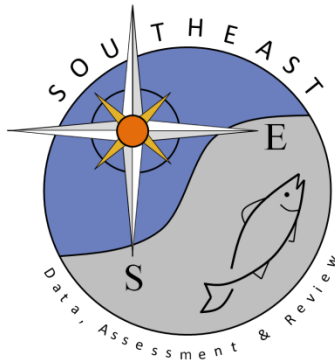


Standardized Video Counts of Southeast US Atlantic Cobia  
(*Rachycentron canadum*) from the Southeast Reef Fish Survey

Lew Coggins, Nathan Bacheler, Kyle Shertzer, and Erik Williams

SEDAR95-DW-01

29 April 2024



*This information is distributed solely for the purpose of pre-dissemination peer review. It does not represent and should not be construed to represent any agency determination or policy.*

Please cite this document as:

Lew, Nathan Bacheler, Kyle Shertzer, and Erik Williams. 2024. Standardized Video Counts of Southeast US Atlantic Cobia (*Rachycentron canadum*) from the Southeast Reef Fish Survey. SEDAR95-DW-01. SEDAR, North Charleston, SC. 19 pp.

# **Standardized Video Counts of Southeast US Atlantic Cobia (*Rachycentron canadum*) from the Southeast Reef Fish Survey**



Lew Coggins, Nathan Bacheler, Kyle Shertzer, and Erik Williams  
SEDAR95-WPXX

Southeast Fisheries Science Center  
National Marine Fisheries Service

April, 2024

Please cite this document as:

Coggins, Lew, Nathan Bacheler, Kyle Shertzer, and Erik Williams. Standardized video counts of southeast US Atlantic Cobia (*Rachycentron canadum*) from the Southeast Reef Fish Survey. SEDAR95-WPXX. SEDAR, North Charleston, SC.

## 1 Abstract

Standardized video counts of cobia (*Rachycentron canadum*) were generated from video cameras deployed by the Southeast Reef Fish Survey during 2011–2022 (note that no sampling occurred in 2020 due to covid-19). The analysis included samples taken between Cape Hatteras, North Carolina and St. Lucie Inlet, Florida, from 14 to 115 m deep. The index is meant to describe the population abundance trend of cobia in the region using a variety of predictor variables that could influence predictions of their abundance and video detection. We compared multiple model structures using AIC and ultimately applied a zero-inflated negative binomial model to standardize the video count data with eight predictor variables. While the final model fit well based on various model diagnostics, the sparsity of cobia observations in the survey resulted in an index with low precision and difficulty estimating the uncertainty of model parameters. The 2011–2022 index values and uncertainty included a calibration factor to account for a change in camera type after 2014.

## 2 Background

The Marine Resources Monitoring, Assessment, and Prediction (MARMAP) program has conducted most of the historical fishery-independent sampling in the U.S. South Atlantic (North Carolina to Florida). MARMAP has used a variety of gears over time, but chevron traps are one of the primary gears used to monitor reef fish species and have been deployed since the late 1980s. In 2009, MARMAP began receiving additional funding to monitor reef fish through the SEAMAP-SA program. In 2010, the SouthEast Fishery-Independent Survey (SEFIS) was initiated by NMFS to work collaboratively with MARMAP/SEAMAP-SA using identical methods to collect additional fishery-independent samples in the region. Together, these three programs are now called the Southeast Reef Fish Survey (SERFS). In 2010, video cameras were attached to some traps deployed by SERFS, and beginning in 2011 all traps included video cameras (Figure 1).

The SERFS currently samples between Cape Hatteras, North Carolina, and St. Lucie Inlet, Florida. This survey targets hardbottom habitats between approximately 15 and 115 meters deep. SERFS began affixing high-definition video cameras to chevron traps on a limited basis in 2010 (Georgia and Florida only), but, since 2011, has attached cameras to all chevron traps as part of their normal monitoring efforts. In 2015, the video cameras were changed from Canon to GoPro to reduce costs and implement a wider field of view, thus observing more fish. A calibration study (detailed below) with both camera types used simultaneously was undertaken to account for differences in fish counts.

Hard-bottom sampling stations were selected for sampling in one of three ways. First, most sites (74.4%) were randomly selected from the SERFS sampling frame that consisted of approximately 4,300 sampling stations on or very near hard bottom habitat. Second, some stations (15.1%) in the sampling frame were sampled opportunistically even though they were not randomly selected for sampling in a given year. Third, new hard-bottom stations were added during the study period through the use of information from various sources including fishermen, charts, and historical surveys (10.5%). These new locations were investigated using a vessel echosounder or drop cameras and sampled if hard bottom was detected. Only those new stations landing on or near hardbottom habitat were included in the analyses. All sampling for this study occurred during daylight hours between April and October on the R/V Savannah, R/V Palmetto, R/V Sand Tiger, or the NOAA Ship Pisces using identical methodologies as described below. Samples were intentionally spread out spatially on each cruise (see Figure 2 in Bachelier and Carmichael (2014)).

Chevron traps were constructed from plastic-coated, galvanized 2-mm diameter wire (mesh size = 3.4 cm<sup>2</sup>) and measured 1.7 m × 1.5 m × 0.6 m, with a total volume of 0.91 m<sup>3</sup>. Trap mouth openings were shaped like a teardrop and measured approximately 18 cm wide and 45 cm high. Each trap was baited with 24 menhaden (*Brevoortia* spp.). Traps were typically deployed in groups of six, and each trap in a set was deployed at least 200 m from all other traps to provide some measure of independence between traps. A soak time of 90 minutes was targeted for each trap deployed.

Canon Vixia HFS-200 high-definition video cameras in Gates underwater housings were attached to chevron traps in 2011–2014, facing outward over the mouth. In 2015, Canon cameras were replaced with GoPro Hero 4 cameras over the trap mouth. Fish were counted exclusively using cameras over the trap mouth. A second high-definition GoPro Hero, Hero 3+, or Hero 4 video or Nikon Coolpix S210/S220 still camera was attached over the nose of most traps in an underwater housing, and was used to quantify microhabitat features in the opposite direction. Cameras were turned on and set to record before traps were deployed, and were turned off after trap retrieval. Trap-video samples were excluded from our analysis if videos were unreadable for any reason (e.g., too dark, camera out of focus, files corrupt) or the traps did not fish properly (e.g., bouncing or dragging due to waves or current, trap mouth was obstructed).

In advance of the switch to GoPro cameras exclusively in 2015, we conducted a calibration study in the summer of 2014 where Canon and GoPro cameras were attached to traps side-by-side and fish were counted at the same time. A total of 54 side-by-side comparisons were recorded. Cobia were observed in only 3 calibration videos, so we used a more general calibration for all paired calibration samples, as recommended by Bacheler et al. (2023). This allowed us to use a robust calibration factor that expanded Canon counts to make them comparable to GoPro counts.

Relative abundance of reef fish on video has been estimated using the MeanCount approach (Conn (2011); Schobernd et al. (2014)). MeanCount was calculated as the mean number of individuals of each species over a number of video frames in the video sample. Video reading time was limited to an interval of 20 total minutes, commencing 10 minutes after the trap landed on the bottom to allow time for the trap to settle. One-second snapshots were read every 30 seconds for the 20-minute time interval, totaling 41 snapshots read for each video. The mean number of individuals for each target species in the 41 snapshots is the MeanCount for that species in each video sample. Zero-inflated modeling approaches described below require count data instead of continuous data like MeanCount. Therefore, these analyses used a response variable called SumCount, which was simply the sum of all individuals seen across all video frames. SumCount and MeanCount track exactly linearly with one another when the same numbers of video frames are used in their calculation (Bacheler and Carmichael (2014)). Therefore, SumCount values were only used from videos where 41 frames were read (94.4% of all samples).

SERFS employed video readers to count fish on videos. There was an extensive training period for each video reader, and all videos from new readers were re-read by fish video reading experts until they were very high quality. After that point, 10% or 15 videos (whichever was larger) were re-read annually by fish video reading experts as part of quality control. Video readers also quantified microhabitat features (e.g., substrate composition), in order to standardize for habitat types sampled over time. Water clarity was also scored for each sample as poor, fair, or good. If bottom substrate could not be seen, then water clarity was considered poor, and if bottom habitat could be seen but the horizon was not visible, water clarity was considered fair. If the horizon could be seen in the distance, water clarity was considered to be good. Including water clarity in index models allowed for a standardization of fish counts based on variable water clarities over time and across the study area. A CTD cast was also taken for each simultaneously deployed group of traps, within 2 m of the bottom, and water temperature from these CTD casts was available for standardization models.

### 3 Data and Treatment

Overall, there were 16,370 survey videos with data available covering a period of 13 years (2011–2022; note no sampling occurred in 2020 due to covid-19). Although data were available from 2010, they were not considered here due to limitations in spatial coverage and a different camera used in that year. For the years considered, several data filters were applied. We removed any data points in which the survey video was considered unreadable by an analyst (e.g., too dark, corrupt video file), or if the trapping event was flagged for any irregularity that could have affected catch rates (e.g., trap dragged or bounced). Additionally, any survey video for which fewer than 41 video frames were read was removed from the full data set. Standardizing the number of readable frames for any data point was essential due to our use of SumCount as a response variable (see above). We also identified any video sample in which corresponding predictor variables were missing and removed them from the final data set. Of the 16,370 video samples considered for inclusion, 2,566 were removed based on the data filtering process described above, leaving

13,804 videos included in the analysis, of which 207 were positive for cobia (1.5% overall). The spatial distribution of the videos included in the analysis cover the area from Cape Hatteras, North Carolina, to St. Lucie Inlet, Florida (Figure 2).

## 4 Standardization

### Response Variable

We modeled SumCount as the response variable. SumCount measured the total number of cobia observed across all 41 frames of each video.

### Explanatory Variables

We considered eight explanatory variables: year, season, depth, latitude, water temperature, turbidity, current direction, and substrate composition. Although all of these explanatory variables were considered, we included in the final formulation only those that improved model performance based on AIC (assuming models converged).

YEAR (*y*) – Year was included because standardized video counts by year are the objective of this analysis. We modeled data from 2011–2022 (excluding 2020 when no sampling occurred). Annual summaries of data points considered are outlined in Table 1.

SEASON (*t*) – Season is a temporal parameter based on the day of the year of sampling (Figure 3). The season parameter is treated as a factor with days distributed among quartiles.

DEPTH (*d*) – Water depth was treated as a factor with four levels based on quartiles (Figure 3). Annual depth distribution for survey data are outlined in Table 1.

LATITUDE (*lat*) – The latitude of video samples (Figure 3) was divided into 4 levels based on quartiles.

TEMPERATURE (*temp*) – The bottom water temperature was collected from cluster of stations and incorporated as a predictor variable. Bottom temperatures ranged from 12.4 to 32.6 degrees Celsius (Figure 3). For the model, temperature was treated as a factor with 4 levels based on quartiles.

TURBIDITY (*wc*) – Turbidity can affect both species distribution and the ability of an analyst to observe and identify species on videos. Turbidity information is recorded during video analysis based on the ability of an analyst to perceive the horizon and surrounding habitat, and it was scored at three levels: poor, fair, and good. Given that poor water clarity occurred rarely and was associated with very few cobia observations, it was removed from all analyses, leaving only fair and good levels.

CURRENT DIRECTION (*cd*) – This categorical variable describes current direction based on the video point of view. Current direction was included to better account for variability in detection due to the current moving fish away or towards the camera. This variable is assigned one of three levels during video processing: away, sideways, or towards.

SUBSTRATE COMPOSITION (*sc*) – Substrate composition is an estimate of the proportion of the visible substrate that is hardbottom and is assigned during video processing. This variable was treated as a categorical variable with 4 levels: none (0%), low (1–9%), moderate (10–39%), and high ( $\geq 40\%$ ).

## 5 Zero-Inflated Model

The recommendation of the video index workshop (Bacheler and Carmichael (2014)) was to apply a zero-inflated modeling approach to the development of fishery-independent video indices. Zero-inflated models are valuable tools for modeling distributions that do not fit standard error distributions due to an excessive number of zeroes. These data distributions are often referred to as “zero-inflated” and are a common condition of count based ecological data. Zero inflation is considered a special case of over-dispersion that is not readily addressed using traditional transformation procedures (Hall (2000); Zeileis et al. (2008)). Due to the high proportion of zero counts found in our data set, we used a zero-inflated mixed model approach that accounts for the high occurrence of zero values, as well as the positive counts. The model does so by combining binomial and count processes (Jackman (2024); Zeileis et al. (2008)).

The modeling approached used here was similar to that used in many previous SEDARs. We initially considered a full null model (1) using both a zero-inflated Poisson (ZIP) and a zero-inflated negative binomial (ZINB) formulation as:

$$Sumcount = y + wc + cd + sc + d + t + lat + temp \mid y + wc + cd + sc + d + t + lat + temp \quad (1)$$

In this formulation, variables to the left of the “|” apply to the count sub-model, and variables to the right apply to the binomial sub-model. We compared the fit and variance structure of each model formulation using AIC and likelihood ratio tests (Zuur et al. (2009)) to determine the most appropriate model error structure for the development of a cobia video index. The results of these tests showed clear support for the ZINB formulation (Table 2). These results concur with our expectations based on the over dispersion of video survey data and with the recommendations of the video index development panel (Bacheler and Carmichael (2014)).

We used a step-wise backwards model selection procedure based on AIC to systematically exclude unnecessary parameters from our full model formulation. We first conducted model selection on the left (count) sub-model with the right (binomial) sub-model specified as intercept only. This resulted in the best model being one that excluded all predictor variables except year ( $y$ ), turbidity ( $wc$ ), and substrate composition ( $sc$ ). We then performed model selection on the right (binomial) sub-model where all covariates were included except latitude ( $lat$ ). Thus, our final ZINB model formulation, based on the results of AIC and likelihood ratio tests (Zuur et al. (2009)), included three predictors on the negative binomial side ( $y$ ,  $wc$ , and  $sc$ ) and seven predictors on the binomial side ( $y$ ,  $wc$ ,  $cd$ ,  $sc$ ,  $d$ ,  $t$ , and  $temp$ ). The data were fit well using the final (best) model (Figure 4). All data manipulations and analyses were conducted using R version 4.3.2 (R Core Team (2023)). Modeling was executed using the `zeroinfl` function in the `pscl` package (Jackman (2024), Zeileis et al. (2008)) available from the Comprehensive R Archive Network (CRAN).

## 6 Calibration of Gear

Because camera gear changed in 2015 (from Canon to GoPro), index values in 2011-2014 were adjusted to make them comparable to values in 2015–2022. Cobia were only observed on 3 videos during the calibration study, so we instead used calibrations from all species. MeanCounts from GoPros cameras were regressed on MeanCounts from Canon cameras to estimate a slope of 1.606 and a standard error of 0.027 (Figure 5). The slope (i.e., calibration factor) was used to adjust the 2011–2014 index values to make them comparable to data from later years.

## 7 Uncertainty

Uncertainty in the index was computed using a bootstrap procedure with  $n = 1,000$  replicates. In each replicate, a data set of the original size was created by drawing observations (rows) at random with replacement. This was done by year, to maintain the same annual sample size as in the original data. The model (Equation 1) was fitted to



each data set, and uncertainty (CVs) was computed. All of the 1,000 runs converged. Uncertainty in the calibration factor was included in the bootstrap procedure by drawing a random value from a normal distribution with a mean of 1.606 and a standard error of 0.027 (estimates from the calibration regression). These values, one for each bootstrap replicate, were used to scale up the 2011–2014 index estimates. Thus, this method accounts for the adjustment in the 2011–2014 estimates, as well as the corresponding uncertainty.

## 8 Results and discussion

The final ZINB model included three predictors on the negative binomial side ( $y$ ,  $wc$ , and  $sc$ ) and seven predictors on the binomial side ( $y$ ,  $wc$ ,  $cd$ ,  $sc$ ,  $d$ ,  $t$ , and  $temp$ ). This final model fit well (Figure 4) and model residuals were reasonable (Figure 6). However, during the model selection process, candidate models frequently had singular design matrices resulting in an inability to estimate parameter variance. This behavior is frequently ascribed to collinearity among covariates. In an attempt to reduce this suspected collinearity, we examined correlation among covariates to potentially exclude covariates with high correlation ( $|r| \geq 0.7$ ; Dormann et al. (2013)). However, no correlations exceeded the threshold. In an additional attempt to reduce collinearity, we substituted all the original covariates with coordinate values of the first 5 dimensions from a multiple factor analysis of the covariates. While this procedure eliminated collinearity among model predictor variables, the design matrices were still singular for some candidate models. Thus, we ultimately concluded the root cause of the model design matrix singularity is the sparsity of cobia observations in the survey data and no model covariate structure was found to eliminate the problem. Additionally, during the bootstrap procedure where the best model was repeatedly refit to data sampled from the original data, model design matrix singularity was again encountered for many of the replicates. We suspect this may have caused the estimated CV about the index trend to be inflated (Table 3; Figure 7).

For cobia, the proportion positive was low and variable over time ranging from the highest in 2015 (2.8%) and lowest in 2012 (0.7%; Table 3). The standardized index was highest in 2017 and CVs for the index were high and variable ranging between 0.33 to 0.97 (Table 3). The standardized and nominal indices tracked each other reasonably well with the largest deviations in 2012 and 2017. The nominal index was within the 95% confidence intervals of the standardized index in all years except 2012 (Figure 7).

The focus of this document is primarily on construction and technical evaluation of an index of cobia from the SERFS video survey covering the geographic area from Cape Hatteras to South Florida. However, the applicability of this index to inform the SEDAR 95 assessment regarding coastwide abundance of cobia is perhaps a more important question and will rely on consideration of cobia biology, movement, geographic range, and other characteristics relevant to the coverage of the SERFS survey. Such consideration should occur within the Index portions of the Data Workshop webinars. An example of why such consideration is appropriate is the recent shift in the distribution of the proportion of recreational angler trip interceptions reporting cobia as indicated by MRIP data (Figure 8). These data suggest that the majority of successful cobia trips may have recently shifted north of the area sampled within the SERFS program and potentially signalling that the SERFS survey may not be an accurate indicator of cobia abundance coast-wide.

## 9 References

- Bacheler, N. M., and J. Carmichael, 2014. Southeast Reef Fish Survey video index development Workshop Final Report. NMFS-SEFSC and SAFMC. SEDAR41-RD23.
- Bacheler, N. M., K. W. Shertzer, Z. H. Schobernd, and L. G. Coggins. 2023. Calibration of fish counts in video surveys: a case study from the Southeast Reef Fish Survey. *Frontiers in Marine Science* **10**. URL <https://www.frontiersin.org/articles/10.3389/fmars.2023.1183955>.
- Conn, P., 2011. An evaluation and power analysis of fishery independent reef fish sampling in the Gulf of Mexico and U. S. South Atlantic. NOAA Tech. Memorandum NMFS- SEFSC-610.
- Dormann, C. F., J. Elith, S. Bacher, C. Buchmann, G. Carl, G. Carré, J. R. G. Marquéz, B. Gruber, B. Lafourcade, P. J. Leitão, T. Münkemüller, C. McClean, P. E. Osborne, B. Reineking, B. Schröder, A. K. Skidmore, D. Zurell, and S. Lautenbach. 2013. Collinearity: a review of methods to deal with it and a simulation study evaluating their performance. *Ecography* **36**:27–46. URL <https://nsojournals.onlinelibrary.wiley.com/doi/abs/10.1111/j.1600-0587.2012.07348.x>.
- Hall, D. B. 2000. Zero-Inflated Poisson and Binomial Regression with Random Effects: A Case Study. *Biometrics* **56**:1030–1039. URL <http://www.jstor.org/stable/2677034>.
- Jackman, S., 2024. pscl: Classes and Methods for R Developed in the Political Science Computational Laboratory. University of Sydney, Sydney, Australia. URL <https://github.com/atahk/pscl/>.
- R Core Team, 2023. R: A Language and Environment for Statistical Computing. R Foundation for Statistical Computing, Vienna, Austria. URL <https://www.R-project.org/>.
- Schobernd, Z. H., N. M. Bacheler, and P. B. Conn. 2014. Examining the utility of alternative video monitoring metrics for indexing reef fish abundance. *Canadian Journal of Fisheries and Aquatic Sciences* **71**:464–471.
- Zeileis, A., C. Kleiber, and S. Jackman. 2008. Regression Models for Count Data in R. *Journal of Statistical Software* **27**:1–25. URL <https://www.jstatsoft.org/index.php/jss/article/view/v027i08>.
- Zuur, A., E. N. Ieno, N. Walker, A. A. Saveliev, and G. M. Smith. 2009. *Mixed Effects Models and Extensions in Ecology with R*. Springer, New York.

Table 1. Number of videos, depth range, latitude range, and day of the year range of samples included in the analyses.

Year	Number of video samples	Depth( $m$ ) range	Latitude ( $^{\circ}$ N) range	Day of the year range
2011	543	15-94	27.23-34.54	140-299
2012	1017	15-105	27.23-35.01	115-284
2013	1114	15-98	27.33-35.01	115-278
2014	1364	16-109	27.23-35.01	114-295
2015	1374	15-110	27.26-35.02	112-296
2016	1409	16-115	27.23-35.01	125-300
2017	1409	15-111	27.23-35.02	117-273
2018	1647	16-114	27.23-35.00	116-278
2019	1538	14-110	27.23-35.01	121-269
2020	0	-	-	-
2021	1373	16-109	27.23-35.01	119-274
2022	1016	16-113	27.23-35.01	117-271

Table 2. Comparison of zero-inflated Poisson and zero-inflated negative binomial models using preliminary (full) model error structure comparison.

Model	df	Likelihood	AIC	$\chi^2$	<i>p</i> -value
ZIP	58	-1841	3797		
ZINB	59	-1467	3052	747.1	<0.0001

Table 3. The relative nominal *SumCount*, number of videos included ( $N$ ), proportion of videos in which cobia were observed (i.e., proportion positive), standardized index, and CVs for the *SERFS* cobia video index, 2011–2022.

Year	Relative nominal <i>SumCount</i>	$N$	Proportion positive	Standardized index	CV
2011	0.233	543	0.009	0.218	0.59
2012	1.967	1017	0.007	0.982	0.92
2013	0.737	1114	0.010	0.599	0.41
2014	0.633	1364	0.015	0.739	0.34
2015	1.660	1374	0.028	1.517	0.32
2016	1.749	1409	0.016	1.283	0.38
2017	1.507	1409	0.017	2.596	0.46
2018	0.939	1647	0.019	1.309	0.36
2019	0.835	1538	0.014	1.012	0.38
2021	0.506	1373	0.012	0.518	0.43
2022	0.232	1016	0.009	0.226	0.49

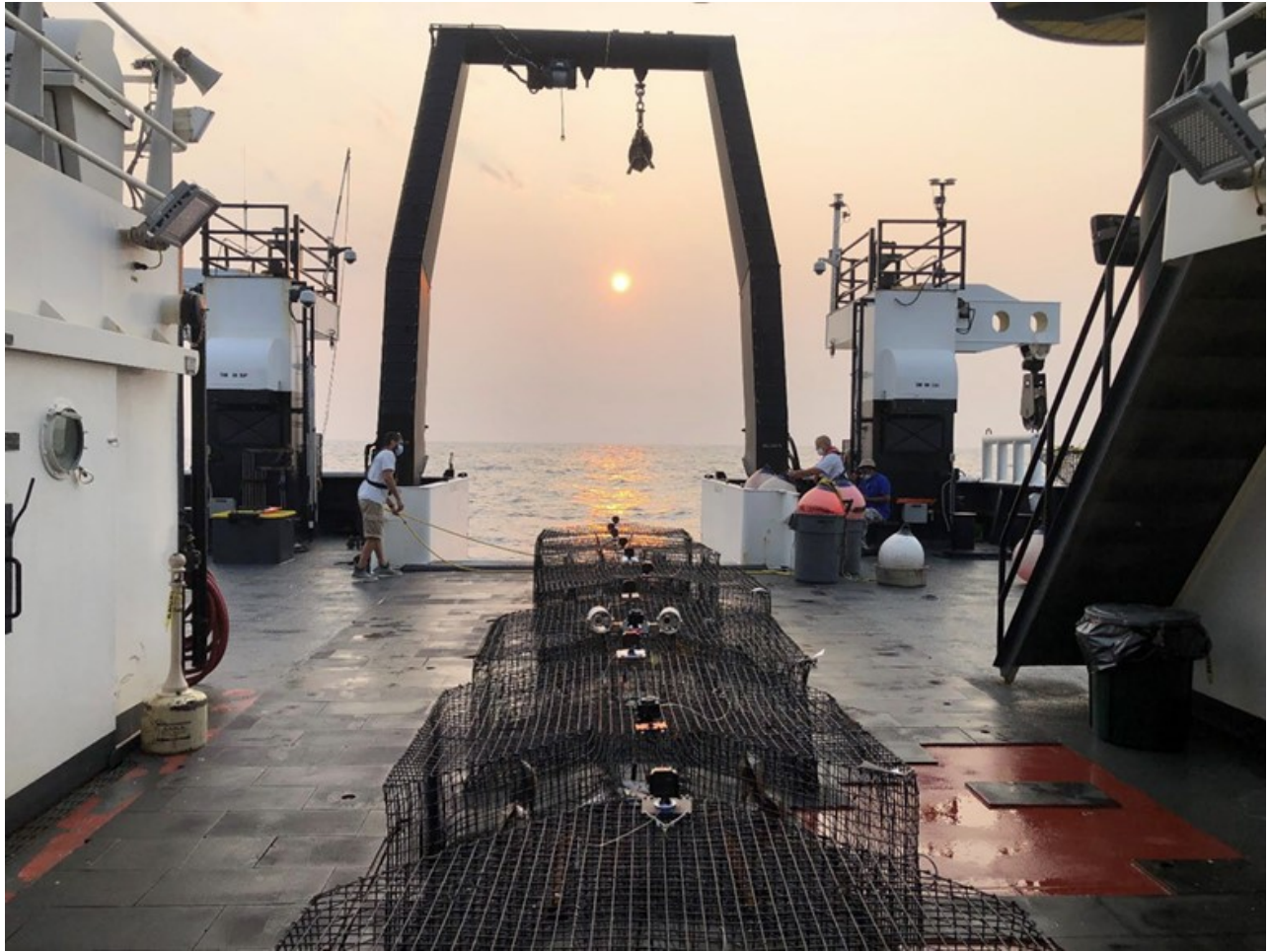


Figure 1 Chevron traps used by SERFS showing the GoPro cameras over the trap mouth and nose.

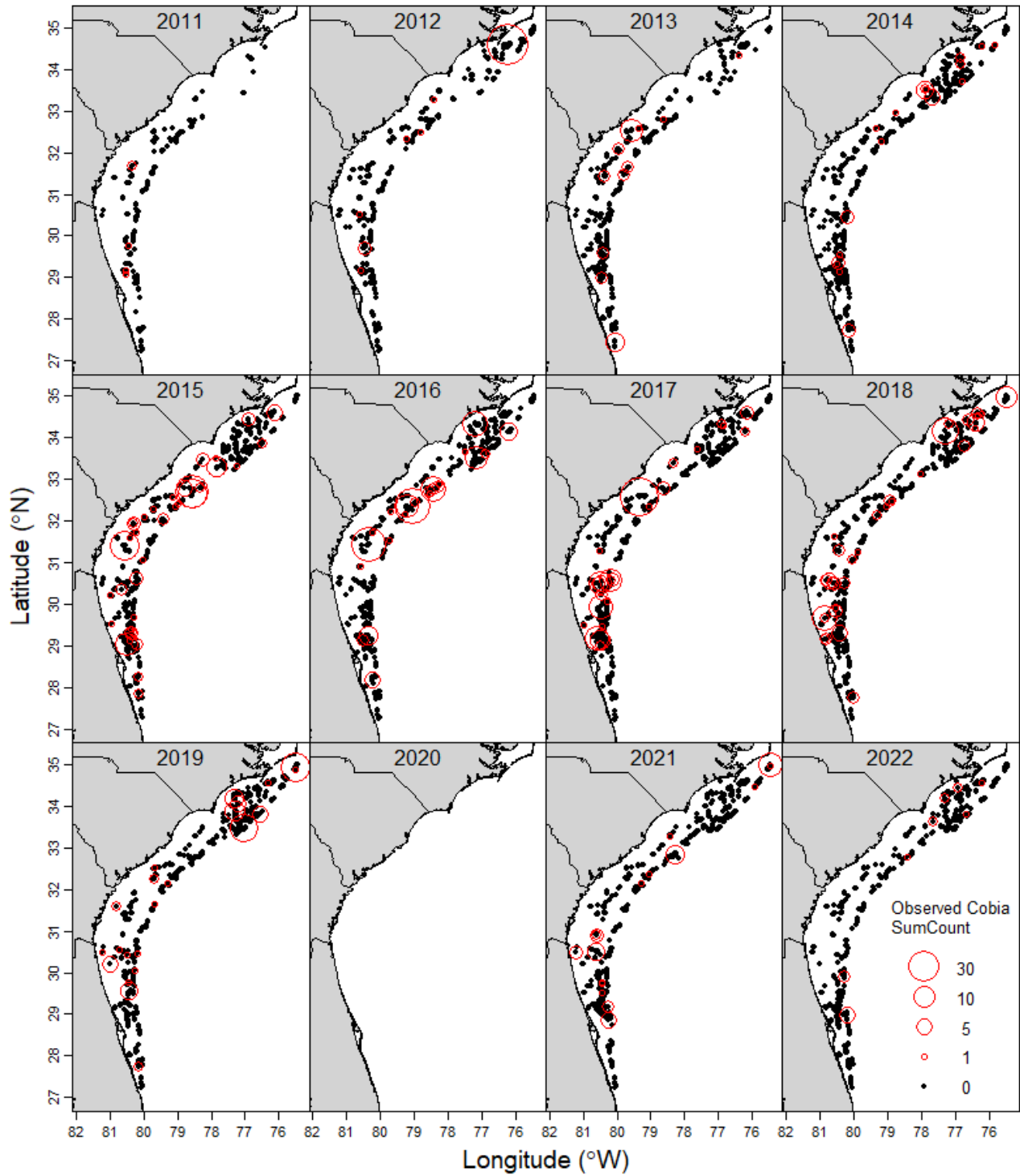


Figure 2 Bubble plots of cobia *SumCounts* from videos collected by the Southeast Reef Fish Survey, 2011–2022. Black points show locations where cobia were not observed on video and red bubbles show where cobia were observed on video, with the size of the bubbles scaled to their video *SumCount*. Note that points overlap often. No sampling occurred in 2020 due to the covid-19 pandemic.

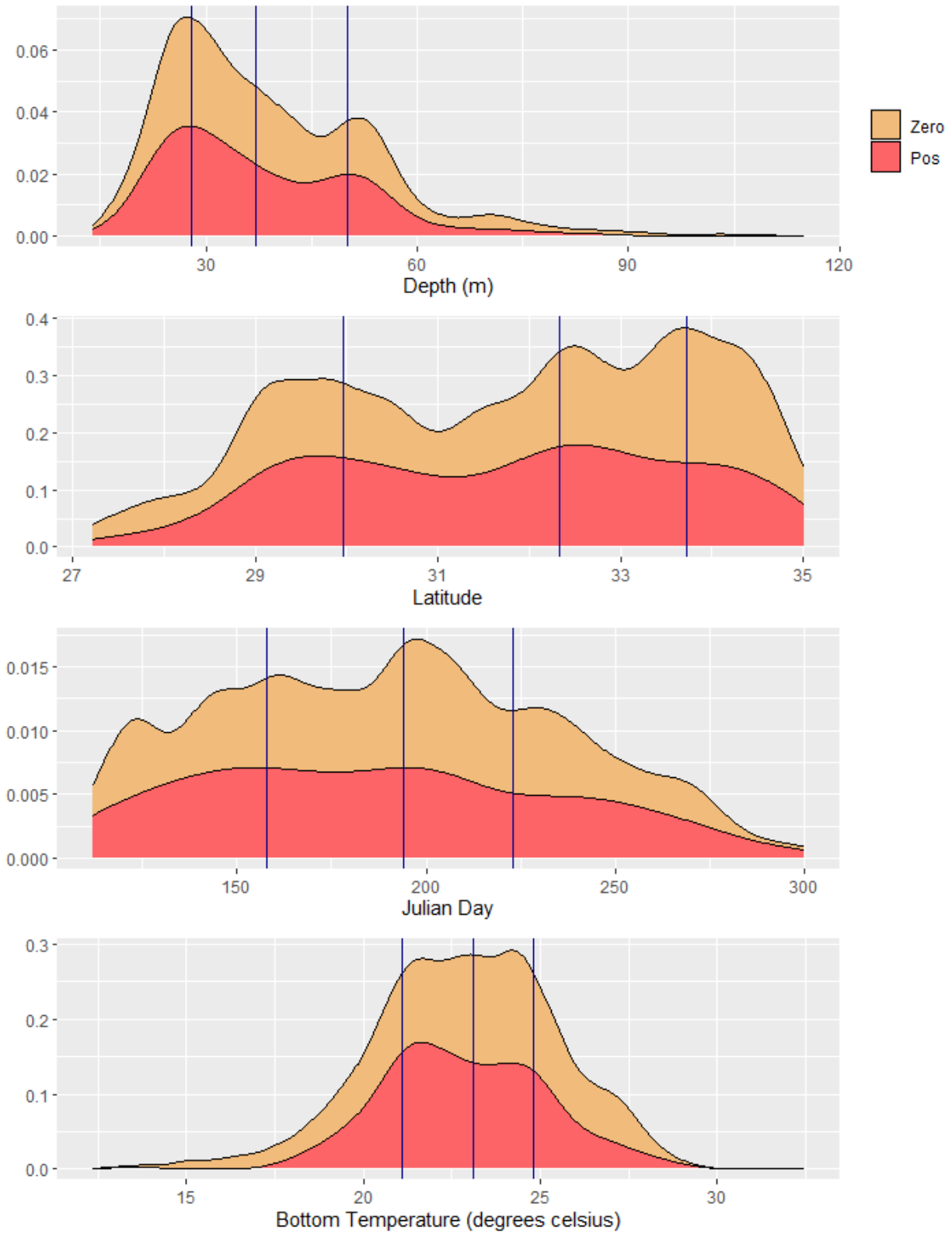


Figure 3 Distribution of data collected as continuous variables for positive (red) and zero (orange) counts. Vertical lines represent break points for factor definitions.



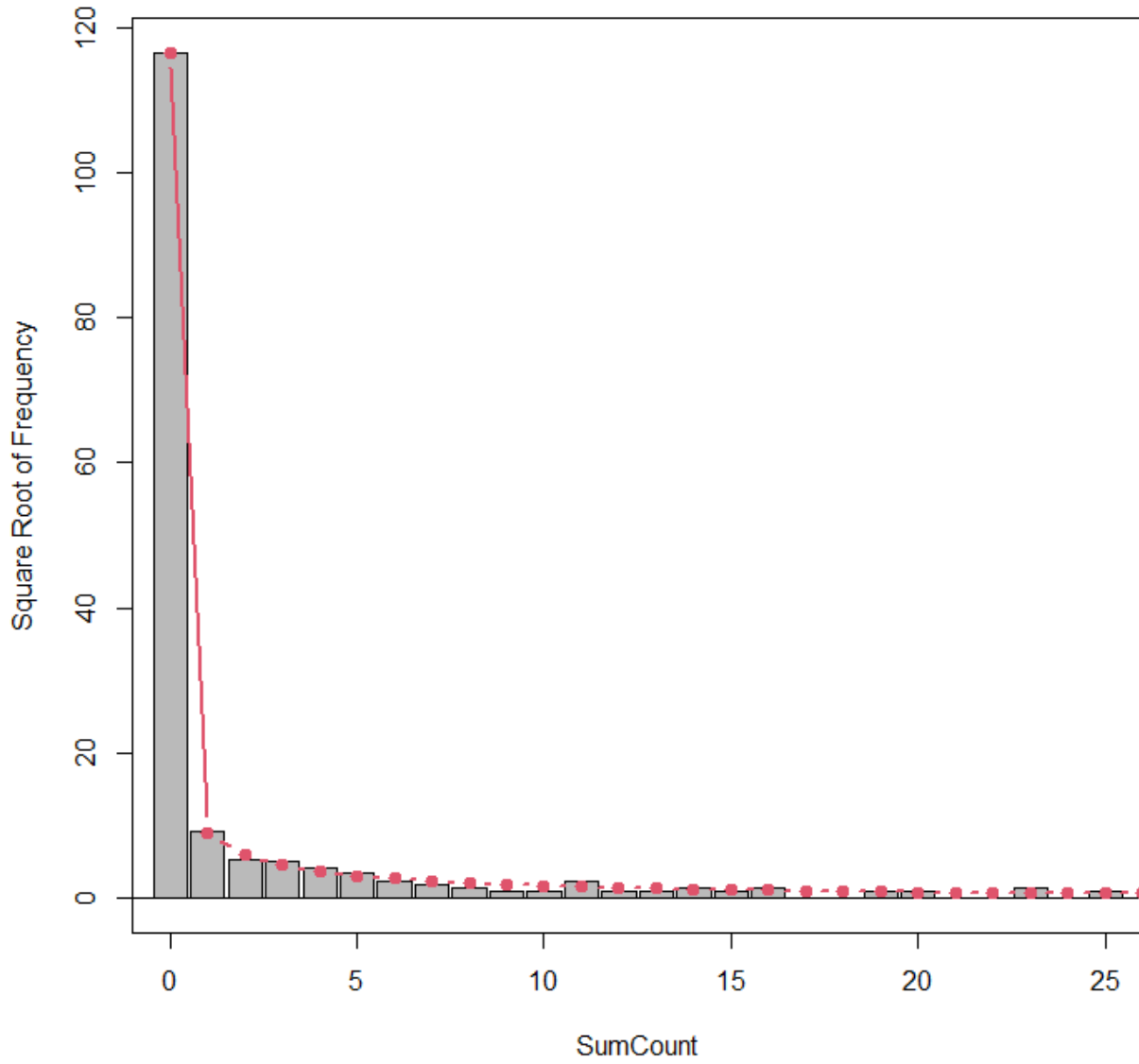


Figure 4 Model diagnostic plot of fitted model values (red line) against the original data distribution for the preferred model for cobia.

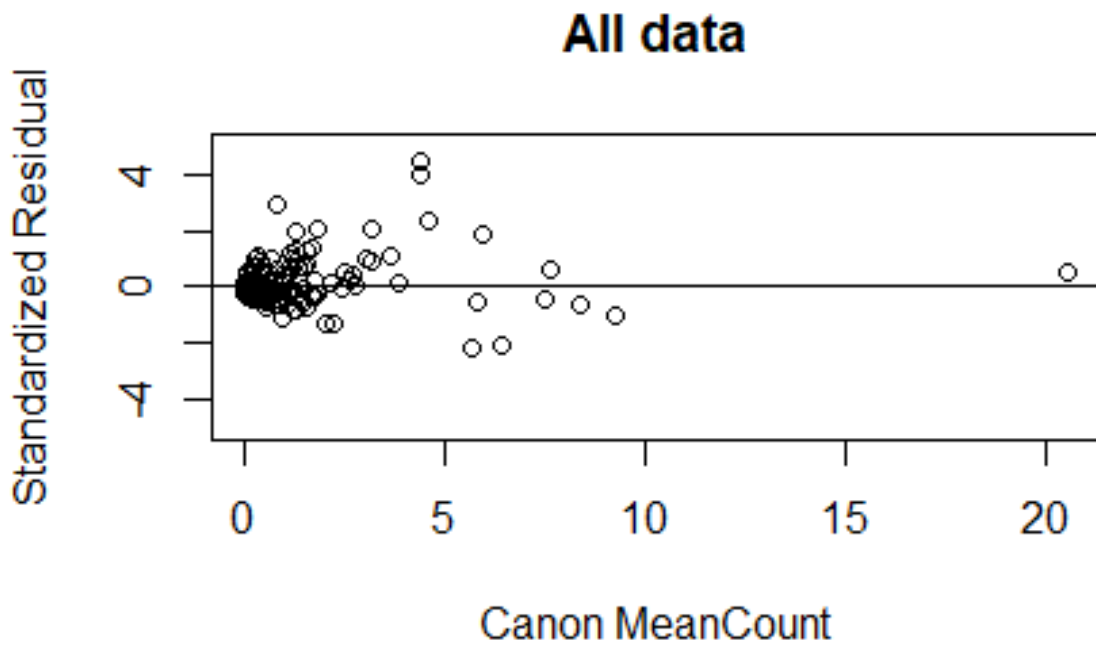
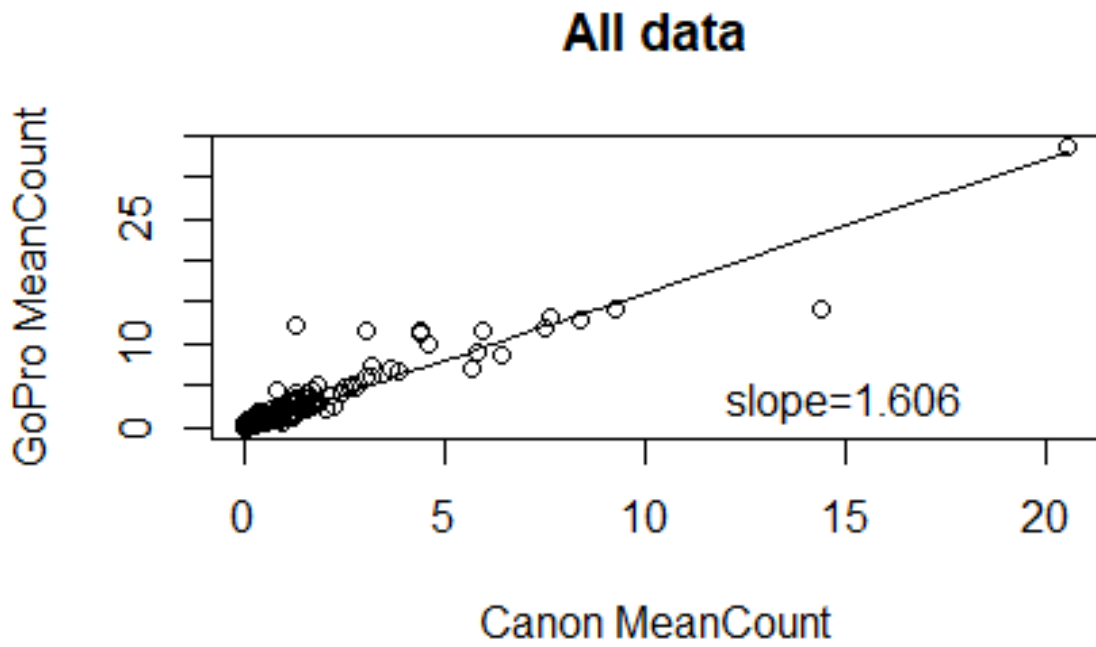


Figure 5 Top row: relationship between all species MeanCounts using GoPro and Canon cameras from the 2014 camera calibration study using all data. Bottom row: standardized residuals from all data.

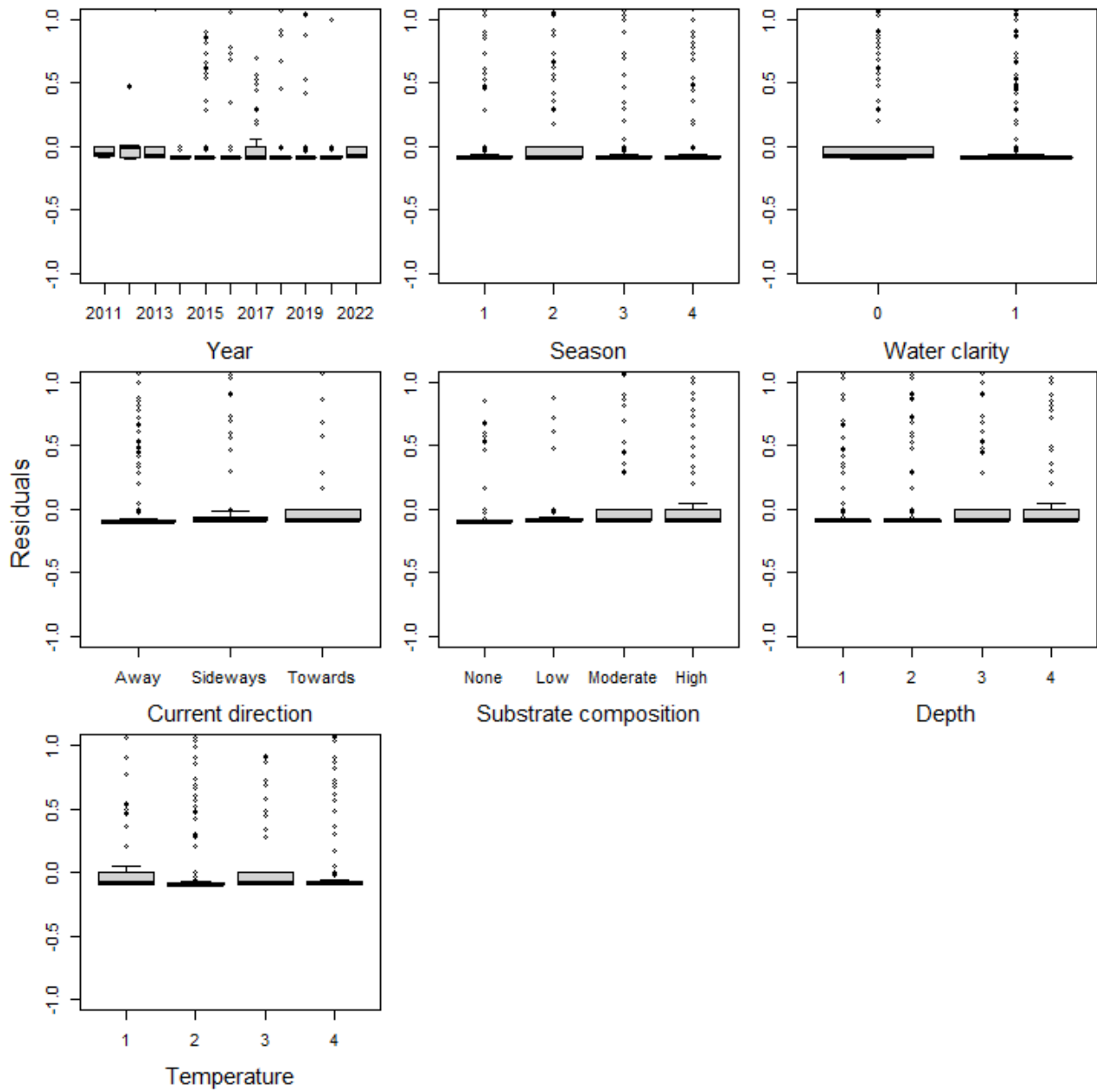


Figure 6 Residuals for all levels of each categorical predictor variable included in the zero-inflated negative binomial model.

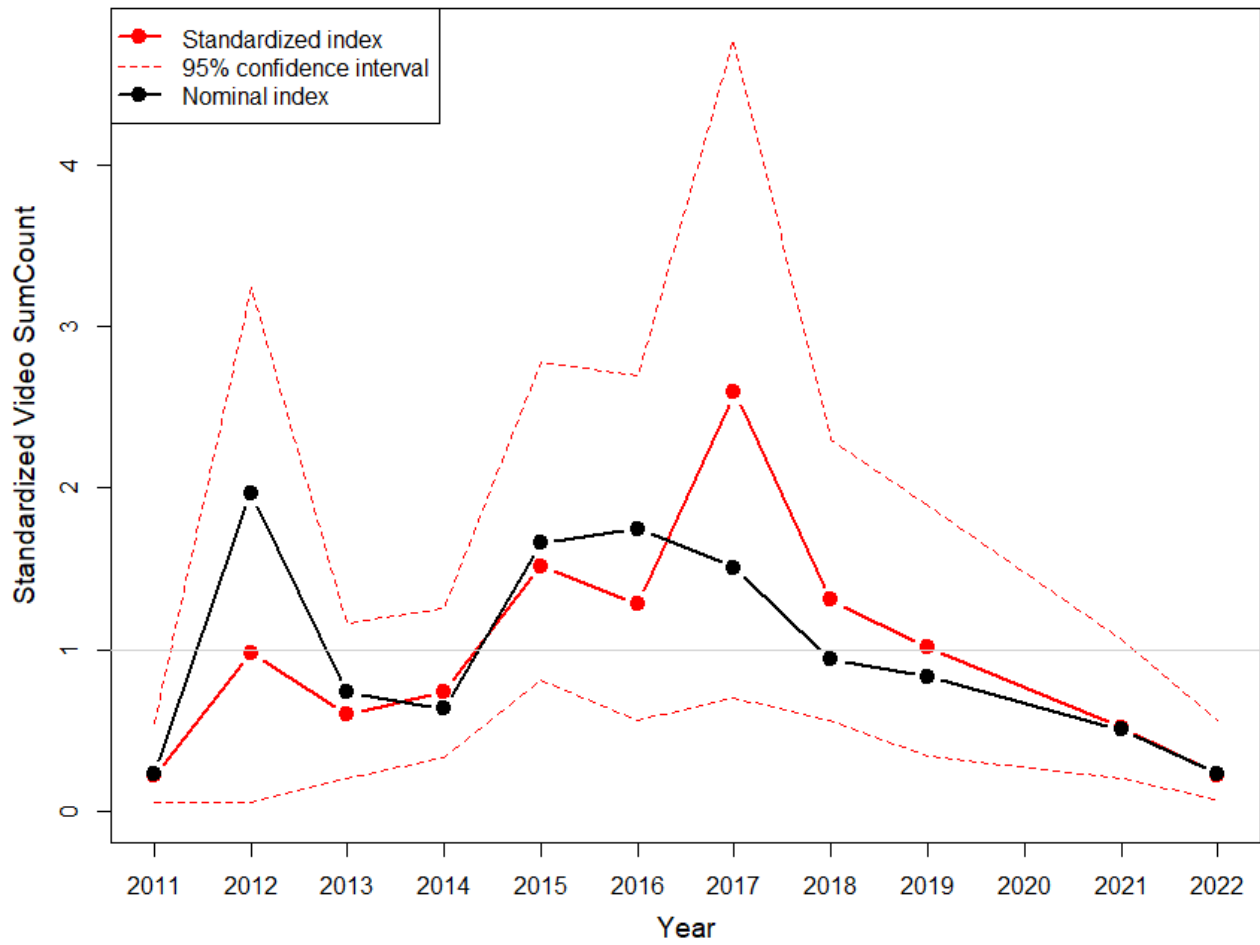


Figure 7 Cobia relative standardized index (red line and points) with 2.5% and 97.5% confidence intervals (red dashed lines) and the relative nominal index (black line with points) from SERFS video data using a zero-inflated negative binomial model.

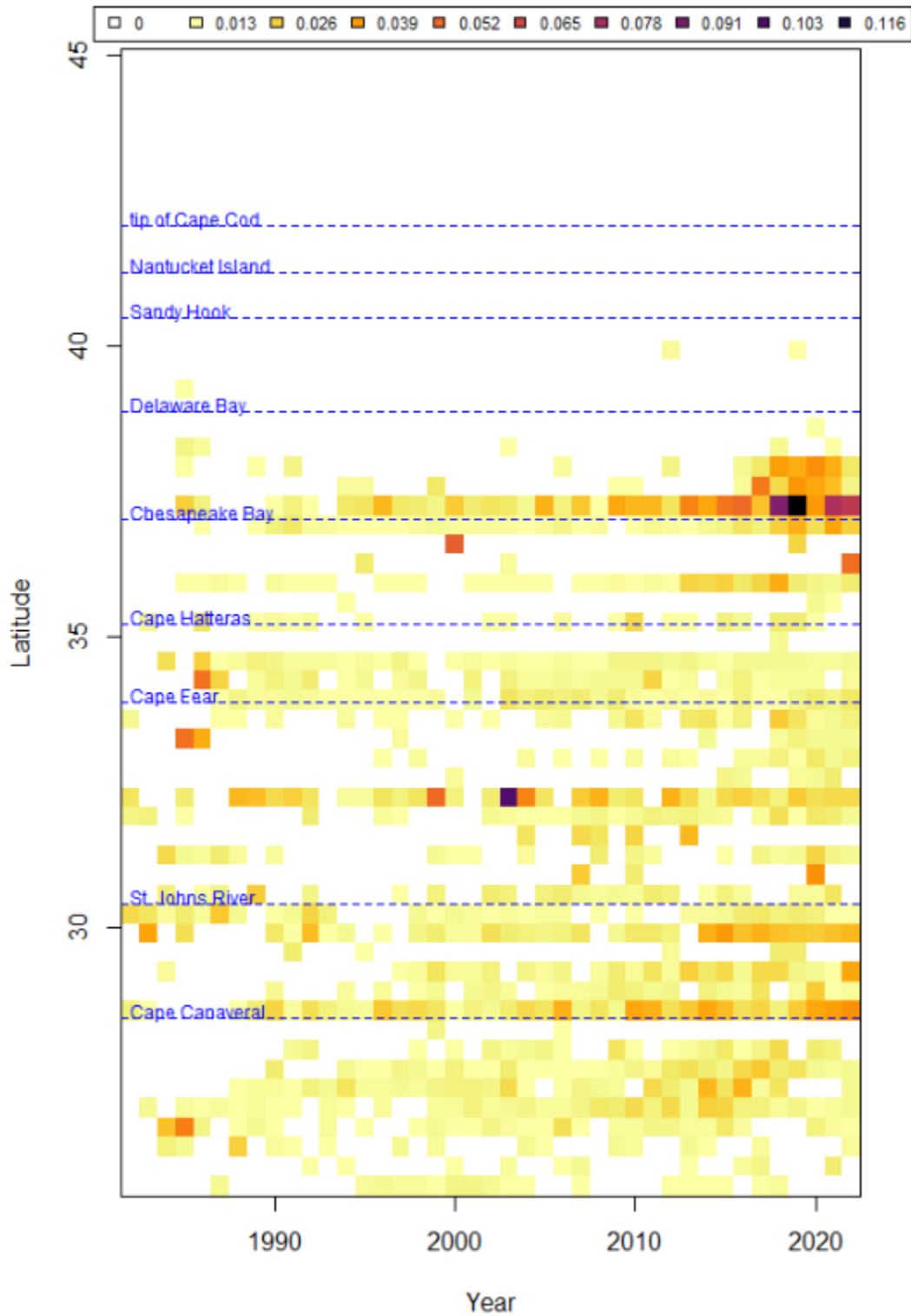


Figure 8 Temporal and spatial distribution of the proportion of recreational angler trip interceptions reporting cobia as indicated by the MRIP program.